This document was prepared in conjunction with work accomplished under Contract No. DE-AC09-96SR18500
with the U. S. Department of Energy.

DISCLAIMER

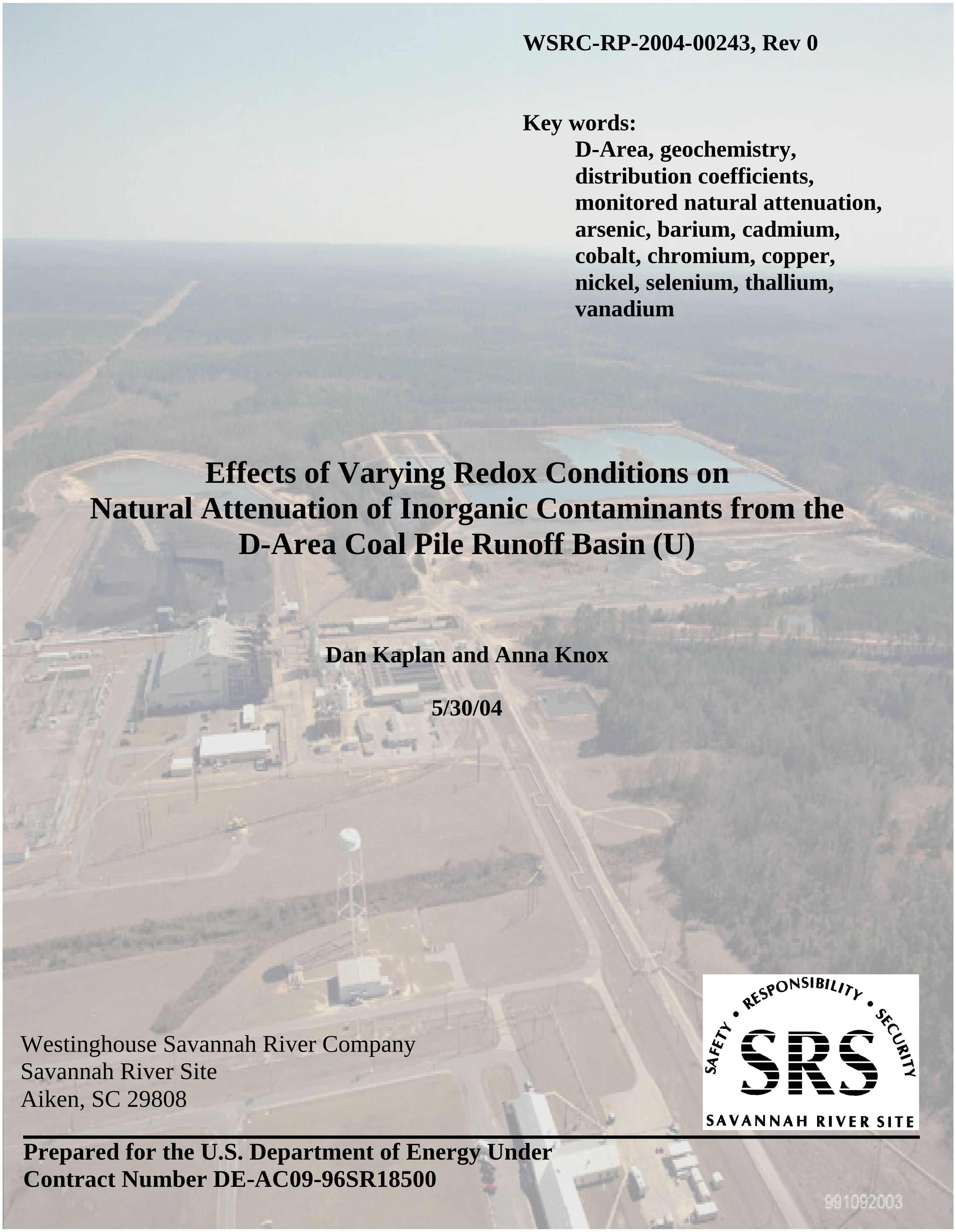

WSRC-RP-2004-00243, Rev 0

Key words:
D-Area, geochemistry,
distribution coefficients,
monitored natural attenuation,
arsenic, barium, cadmium,
cobalt, chromium, copper,
nickel, selenium, thallium,
vanadium

Effects of Varying Redox Conditions on Natural Attenuation of Inorganic Contaminants from the D-Area Coal Pile Runoff Basin (U)

Dan Kaplan and Anna Knox

5/30/04

Westinghouse Savannah River Company
Savannah River Site
Aiken, SC 29808

Prepared for the U.S. Department of Energy Under
Contract Number DE-AC09-96SR18500

DISCLAIMER

Printed in the United States of America

Prepared For
U.S. Department of Energy

WSRC-RP-2004-00243, Rev 0

Key words:
D-Area, geochemistry,
distribution coefficients,
monitored natural attenuation,
arsenic, barium, cadmium,
cobalt, chromium, copper,
nickel, selenium, thallium,
vanadium

Effects of Varying Redox Conditions on Natural Attenuation of Inorganic Contaminants from the D-Area Coal Pile Runoff Basin (U)

Dan Kaplan and Anna Knox

5/30/04

Westinghouse Savannah River Company
Savannah River Site
Aiken, SC 29808

Prepared for the U.S. Department of Energy Under
Contract Number DE-AC09-96SR18500

REVIEWS AND APPROVALS

Daniel I. Kaplan 5/30/04

Daniel I. Kaplan, Author, Waste Processing Technology Date

Anna S. Knox

Anna S. Knox, Author, Environmental Science and Technology Date

B. T. Butcher 1/5/05

Byron T. Butcher, Level 4, Waste Processing Technology Date

William E. Stevens 1/12/05

William E. Stevens, Authorized Derivative Classifier, Waste Processing Technology Date

Adrian Pishko 12/9/04

Adrian Pishko, Design Check, Waste Processing Technology Date

Kimberly P. Crapse 1/14/05

Kimberly P. Crapse, Reviewer, Waste Processing Technology Date

TABLE OF CONTENT

LIST OF ACRONYMS

COCs	constituents of concern
DCPRB	D-Area Coal Pile Runoff Basin
K_d	distribution coefficient
SHE	standard hydrogen electrode
SRTC	Savannah River Technology Center
ICP-AES	inductively couple plasma – atomic emission spectroscopy
ICP-MS	inductively couple plasma – mass spectroscopy

LIST OF FIGURES

LIST OF TABLES

1.0 Abstract

The objective of this study was to provide geochemical parameters to characterize the D-Area Coal Pile Runoff Basin (DCPRB) sediment as a potential source term. It is anticipated that the measured values will be used in risk calculations and will provide additional technical support for imposing Monitored Natural Attenuation at D-Area. This study provides a detailed evaluation of the DCPRB sediment and is part of another study that quantified the Monitored Natural Attenuation of inorganic contaminants more broadly at the D-Area Expanded Operable Unit, which includes the DCPRB (Powell et al. 2004). Distribution coefficients (K_d values; a solid to liquid contaminant concentration ratio) and the Potentially Leachable Fraction (the percent of the total contaminant concentration in the sediment that can likely contribute to a contaminant plume) were measured in a DCPRB sediment as a function of redox conditions. Redox conditions at the DCPRB are expected to vary greatly as the system undergoes varying drying and flooding conditions. Conservative values; K_d values that err on the side of being too low and Potentially Leachable Fraction values that err on the side of being too high) are presented below.

Constituent	K_d	Potential Leachable Fraction	Constituent	K_d	Potential Leachable Fraction
	(mL/g)	(wt-%)		(mL/g)	(wt-%)
As	290	27	Cu	20	100
Be	Soil Be below Det. Limit		Ni	60	76
Cd	60	47	Se	80	36
Co	40	73	Tl	80	100
Cr	110	73	V	860	53

The K_d values are high compared to conservative literature values, and underscores the importance of measuring site-specific values to provide estimates of sediments' natural attenuation/sorption capacities. The Potentially Leachable Fraction indicates that as little as 27% of the As, but all of the Cu and Tl will be part of the source term. In the case of the As, the remaining 83% will likely never leach out of the sediment, thereby providing a form of natural attenuation. Importantly, Be, Cr, Cu, Ni, and V concentrations in the sediment were less-than twice background levels, indicating this sediment was not a potential source for these contaminants. K_d values generally increased significantly (As, Cd, Co, Cr, Cu, Ni, Se, and Tl) when the sediment was flooded and after 36 days biostimulated through the addition of molasses. However, the contaminants that were newly sorbed tended to bind to weaker binding sites as the system was converted from an oxidizing to a reducing system. This redistribution of contaminants resulted in increased Potentially Leachable Fractions. In conclusion, these tests clearly indicate that the DCPRB sediment has a relatively high affinity to sorb most of the contaminants and that when evaluating the risk associated with this as a source term that only the Potentially Leachable Fraction of the total sediment contaminants' concentration be used as the actual source term.

2.0 Introduction

2.1 Desorption Distribution Coefficients

The distribution coefficient, or K_d value, is one of the simplest constructs that describes contaminant sorption to sediments. It is the ratio of the contaminant concentration sorbed to the solid phase divided by the contaminant concentration in the liquid surrounding the solid phase (Eq. 1):

$$K_d = \frac{C_{solid}}{C_{liquid}} \qquad (1)$$

where C_{solid} (mg/kg) and C_{liquid} (mg/L) are the contaminant concentration in the solid and liquid phases, respectively. The K_d value is commonly used to define the retardation factor, which is the ratio of the average linear velocity of water (m/s) divided by the average linear velocity of the contaminant (m/s). The K_d value is related to the retardation factor (*Rf*, unitless) by the bulk density (ρ_b, kg/m) and the porosity (η, m^3/m), as shown in Eq. 2 (Valocchi 1984; Bouwer 1991):

$$Rf = \left(1 + \frac{K_d \rho_b}{\eta}\right). \qquad (2)$$

There are several implicit assumptions involved in using the K_d value in Eq. 2 (Bouwer and Krupka et al. 1999). Among these assumptions is that the rate of sorption is equal to the rate of desorption. In natural sediments, this is rarely the case because desorption processes are almost always appreciably slower than the sorption process. Furthermore, the longer a contaminant is in contact with the sediment, the greater the sorption/desorption hysteresis. For example, Moore and Millward (1988) reported that Th desorption rates were appreciably greater for young than for aged seawater mineral particles. Also Nyffeler, et al. (1984) reported that Th K_d values increased as the contact time between dissolved Th and the solid phase increased. The explanation for this aging effect is that over time, sorbed radionuclides 1) diffuse deeper into the solid-phase structure, or 2) become increasingly occluded under surface-precipitated layers. This latter process is especially common in carbonate systems (Veizer 1983) and may also occur in systems containing Fe- and Al-oxide systems, such as those present at the DCPRB and throughout the SRS. Consequently, K_d values measured via sorption laboratory methods are appreciably less than K_d values measured via desorption methods.

K_d values measured by sorption methods, henceforth referred to as sorption K_d values, are measured and used appreciably more often than desorption methods. This most likely stems from the appreciably greater ease of conducting sorption experiments versus desorption experiments. However, sorption experiments tend not to capture many of the processes controlling contaminant transport as well as desorption experiments. For example, most sorption processes occur in the time frame of seconds to weeks. Natural desorption processes occur in the time frame of years to hundreds of years, which is similar to the time frame of interest for most transport modeling efforts. Perhaps just as important, desorption, as compared to sorption, is often the rate limiting process governing geochemical behavior in sediments. This latter point is important because it implies that contaminant transport is more likely controlled by the slower desorption step rather than by adsorption step.

In contrast to the sorption K_d approach, desorption K_d values are appreciably more difficult to measure. One of the major difficulties lies in defining the contaminant concentration associated with the solid phase, C_{solid} in Eq. 1. The assumption in the K_d construct is that sorption is linear and completely reversible. The term "linear" indicates that the aqueous contaminant concentration does not influence the degree of sorption. The term "reversible" indicates that the rate of sorption is equal to the rate of desorption. The value used in the numerator of a K_d, C_{solid}, must reflect not the total amount of contaminant in the sediment, but the reversibly sorbed contaminant concentration. As examples, contaminants that have become incorporated into the mineral structure or have coprecipitated from solution are clearly no longer at equilibrium with the dissolved species via ion exchange and, hence, should not be included as part of the sorbed C_{solid} when calculating desorption K_d values. If non-reversibly sorbed solid-species are included in the definition of $C_{solid,}$ then K_d values calculated from these data will lead to a systematic overestimation of the true K_d value. Hence, to provide conservative K_d values, one should err on the side of underestimating the contaminant concentration on the solid phase, C_{solid}. (Discussion and comparison of the *in situ* K_d values measured by Powell et al. (2004) is presented in Section 4.2).

It is common for a contaminant to sorb by several processes at the same time when put in contact with a natural heterogeneous sediment. Furthermore, the rate that a contaminant sorbs and desorbs from an assembly of solid phases in a natural sediment varies. For example, cation exchange generally occurs appreciably faster than precipitation. Also, sorption and desorption rates of many cation exchange reactions are almost identical (Serne and LeGore 1996), whereas sorption and desorption rates of surface complexation reactions typically exhibit a greater hysteresis, i.e., the sorption reaction is generally faster than the desorption reaction.

Numerous studies have been conducted to identify extraction techniques that selectively desorb specifically defined sediment fractions (Tessier et al. 1979; Miller et al. 1986; Nirel and Morel 1990; Clark et al. 1996; Kaplan and Serkiz 2001). Typically, contaminants are desorbed from sediments by a sequential series of progressively more-aggressive extractants. Each extractant targets either a particular sorption process, such as cation exchange, or a particular phase within the heterogeneous sediment sample, such as the organic or amorphous Fe-oxide phase. Importantly, these selective or sequential extraction techniques have experimental limitations (Tessier et al. 1979; Nirel and Morel 1990). Problems with sequential extractions include incomplete extraction of trace elements, non-selectivity of extraction reagents for given soil phases, or readsorption of extracted contaminants onto other surfaces (Nirel and Morel 1990). Thus, individual sequential extraction phases may not adequately represent the discrete soil phase to which the contaminant is bound. The point of this discussion is to underscore the operational, as compared to thermodynamic or spectroscopic, nature of these measurements.

2.2 Geochemical Changes that Take Place When Sediments are Submerged Under Water

When a sediment is initially submerged under water, a number of chemical and microbiological changes take place. The first chemical parameter to change is the sediment reduction potential, or redox status. In generalized terms, the redox status can be thought of as the activity (similar to concentration) of free electrons in a system. The greater the free electron activity, the more reduced the system. Conversely, the lower the free electron activity, the more oxidized the system. The reduction potential, or Eh, has units of volts. At pH 5.5, which is the approximate background pH near the DCPRB, the redox status can be divided into three parts that correspond to oxic sediments (Eh > 360 mV), suboxic sediments (180 mV > Eh < 360 mV), and anoxic sediments (Eh < 180 mV) (Sposito 1989). Suboxic sediments differ from oxic sediments in having Eh values low enough to deplete O_2(g), but not low enough to deplete sulfate (this concept will be expanded upon below).

The most important naturally occurring elements affected by sediment redox reactions are C, N, O, S, Mn, and Fe. In the contaminated portion of the DCPRB site, this list grows to include As, Cr, Se, and U. If a sediment is behaving effectively like a closed system (e.g., a flooded sediment under stagnant ponding) and abundant sources of carbon and energy are available to support microbially mediated catalysis, there is a well-defined elemental sequence of reduction reactions. At pH 5.5, this sequence is:

$$O^{-II},\ N^{V},\ Cr^{VI},\ As^{V},\ U^{VI},\ Mn^{IV},\ Fe^{III},\ Hg^{II},\ S^{VI},\ \text{and then organic matter,} \qquad (3)$$

where the Roman numeral superscipts indicate the oxidation state of the oxidant. For the purposes of this review, the most important point to take away from the above sequence is that organic matter is an electron donor and is the last sediment constituent to be reduced. Organic matter concentrations under natural conditions, generally build up in water-saturated sediments because there is little in the sediment system to oxygenate (degrade) it. However, this may not be the case in the DCPRB. It is quite likely that the top soil, containing relatively high concentrations of organic matter, was scraped off during construction of the basin, thereby removing much of the natural reductant capacity. Furthermore, the high acidity of the basin water would enhance organic matter oxidation (degradation), further diminished the tendency of naturally occurring organic matter to accumulate. Therefore, based on these considerations, one might expect that under flooded conditions the DCPRB would not reduce sulfate to sulfide. To achieve that, another carbon source would have to be introduced, such as molasses, and of course, sulfate reducing microbes must be present. The population distribution of microbes, including sulfate reducers, near the DCPRB and D-Area impacted aquifer are presented in Powell et al. (2004).

Figure 1 shows the typical sequence of reduction processes in flooded pH-7 sediment as observed in a silty sediment amended with straw, an organic matter source, and incubated in suspension without oxygen supply for one week (Turner and Patrick 1968). During the first day, the content of dissolved oxygen dropped to a negligible value, and the redox potential decreased from 400-mV to 270-mV. The dissolved oxygen concentrations decrease because sediment microbes (aerobes) prefer to use it instead of other elements as an electron acceptor and the dissolved oxygen is very slowly replenished into the water saturated sediments from the atmosphere. Dissolved oxygen in the atmosphere diffuses into water saturated sediments appreciably slower than in air-filled sediments; the diffusion rate of dissolved oxygen is 10,000 times greater through the gas phase than through the aqueous phase. Furthermore, the solubility of oxygen in water is quite low (about 8-mg/L at 25°C and at sea level), resulting in microbes quickly exhaust the dissolved oxygen in a water-saturated sediment. The depletion of nitrate begins shortly before oxygen disappears. Nitrate is reduced to nitrite, ammonia, and nitrogen gas.

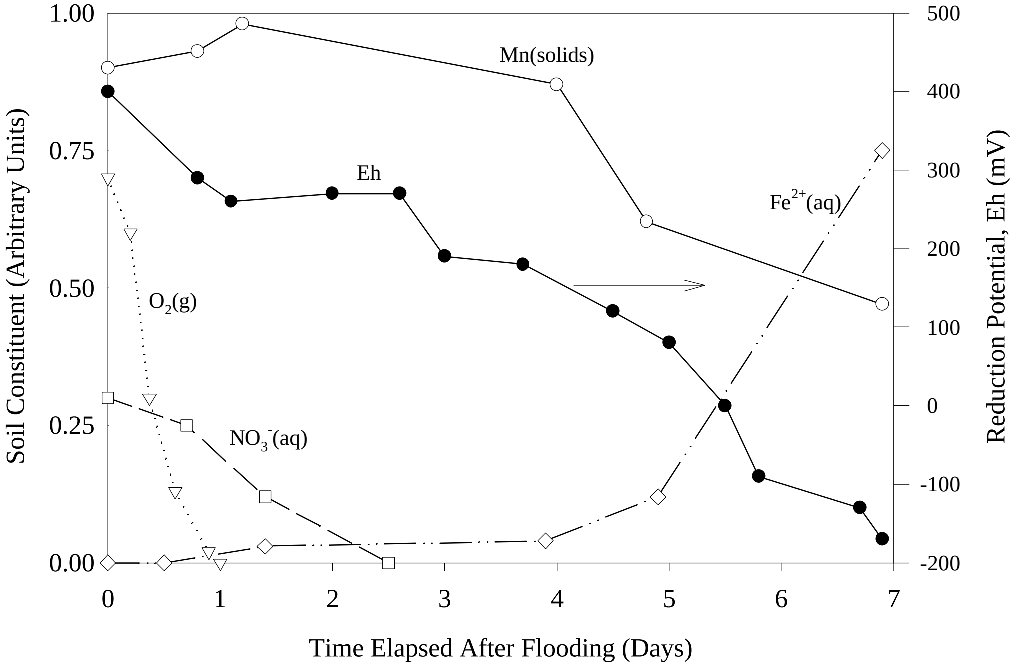

Figure 1. Relative changes in O(g), NO_3^-, $Mn^{III/IV}$ solid phases, and Fe^{2+} content of a sediment with time elapsed after flooding. Changes in reduction potential are also shown and labeled on the right side (Turner and Patrick 1968).

2.2.1 Fe- and Mn-Oxide Dissolution Under Reducing Conditions

Once the sediment system Turner and Patrick (1968) studied obtains a reduction potential of <300 mV, or 1.5-days after becoming water saturated, the Mn solids start to dissolve (Figure 1). Similarly, but at an appreciably lower reduction potential, <180 mV, or 4-days after becoming water logged, the sediment Fe-oxides start to dissolve. These reactions have a number of profound indirect effects on contaminant mobility.

Besides the increase in aqueous Mn and Fe concentrations expected from the lowered reduction potential, a marked increase in the sediment solution concentrations of metals like Cd and Pb, and of ligands like $H_2PO_4^-$ or $HMoO_4^-$ have been observed (Christensen et al. 2000). At the DCPRB and elsewhere on the SRS, dissolved Al concentration would also be expected to greatly increase since Al substitutes for as much as 10% of the Fe in the Fe-oxide structure (Anderson et al. 1993). The principal cause of this secondary phenomenon is the desorption of metals and ligands that occurs when the absorbents to which they are bound become unstable and dissolve. Typically, the metals released in this fashion, are soon readsorbed by solids that are stable at low redox (e.g., clay minerals or sediment organic matter). The contaminants are originally held very strongly onto or in the Fe and Mn solid structures and upon readsorption, may be held less strongly by cation or anion exchange onto the non-dissolved solids. These changes in how strongly the contaminants are held by the solid phases have an obvious influence on the bioavailability and mobility of the contaminants.

In summary, the effect of Mn- and Fe-solid phase dissolution on contaminant mobility is that it:

- decreases the total number of contaminant sorption sites,
- decreases the proportion of strong sorption sites (co-precipitated, precipitated, and occluded phases) in the sediment,
- releases sorbed contaminants into the mobile aqueous phase, and
- releases high concentrations of Al, Fe, and Mn into the aqueous phase that will compete with trace-level contaminants for exchange sites.

Balistrieri et al (1981) found a linear correlation between the apparent adsorption equilibrium constant for metal adsorption to Fe-oxides (specifically the Fe-oxide, goethite) and the hydrolysis constants of that specific metal ion (which are readily available from textbooks). Based on this correlation, one would expect that Cd, Co, Cr, Cu, and Ni, would form much stronger surface complexes with Fe-oxides than As (as either arsenate or arsenite), Be, Se, Tl or V.

2.2.2 Formation of Sparingly Soluble Sulfide Phases Under Reducing Conditions

As noted in Section 2.2, it may not be possible for sulfides to form under the existing conditions in the DCPRB because of the oxidizing nature of the acids and the lack of a strong reductant, such as naturally occurring organic matter. However, under strongly reducing conditions, sulfate ($S^{VI}O_4^{2-}$) is reduced to sulfide (S^{-II}). Sulfides can form sparingly soluble solids with a number of soft metals,[1] such as Cd^{2+}, Cu^+, Pb^{2+},and Tl^+ (Stumm and Morgan 1996). For example, even though Hg exists in concentrations as high as 30 mg/kg in the Inner Swamp sediment of the TNX Outfall Delta operable unit, it is not bioavailable (Specht 1999) and it exists in part-per-billion levels in the sediment porewater (Kaplan and Serkiz 2000). The Hg exists in the sediment almost entirely as mercury sulfide (meta-cinnabar, HgS), a very stable, sparingly soluble form of Hg (Kaplan et al. 1999). Sulfide does not form sparingly soluble precipitates with hard metals, such as Be^{2+} and $U^{VI}O_2^{2+}$ (Stumm and Morgan 1996).

---

[1] Metals and ligands can be classified into 3 categories based on the types of elements they form stable complexes with: hard, soft, or borderline. Soft metals (Zn^{2+}, Pb^{2+}, Cd^{2+}, Hg^{2+} and other elements that have large atomic number to valence state ratios) and soft ligands (P, S, and I) tend to form strong complexes. Similarly, hard metals (e.g., Na^+, K^+, Mg^{2+}, Ca^{2+}, UO_2^{2+}, Ra^{2+}, Mn^{3+}, etc.) and hard ligands (e.g., anions containing O, including NO_3^-, SO_4^{2+} and F^-) tend to form strong complexes. Hard metal – hard ligand bonds tend to be entirely electrostatic, whereas soft metal – soft ligand bonds tend to have a covalency quality to them.

2.2.3 pH Changes as a Sediment Becomes Reduced

When a sediment is submerged, the sediment pH is influenced by a number of reactions (Yu 1991). The impact of these reactions on sediment pH changes as the redox status changes. In general, reduction reactions in aqueous systems take up protons, or make the sediment more basic:

$$A_{ox} + H^{+(aq)} + e^{-}(aq) = A_{red} + H_2O(aq) \qquad (4)$$

where A is some chemical species in any phase [e.g., CO_2(g) or Fe^{2+}(aq), or FeOOH)] and “ox” and “red” designate oxidized and reduced species, respectively. Based on Eq. 4, as an electron, e^-, reduces an oxidized species, A_{ox}, a proton is utilized to form water. For example, 4 protons are consumed when $Mn^{IV}O_2$ is reduced to Mn^{II}; 3 protons are consumed when $Fe^{III}(OH)_3$ (Fe-oxide) is reduced to Fe^{2+} (Fe^{II}); and 10 protons are consumed when $S^{VI}O_4^{2-}$ is reduced to H_2S^{II}.[2] An alternative way of thinking of this pH neutralizing process is that as the Fe and Mn oxide are reduced, hydroxides are released. A number of proton-generating reactions also occur during the reduction process. For instance CO_2 and organic acids are produced through microbiological activities.

Yu (1991) showed that the pH of acidic sediments tends to increase after they are submerged. The pH of a sediment that was originally pH 4.5, increased to near 5.5 after one week and than stabilized after about 2 weeks at a pH of 6.4. Upon adding organic matter to this sediment, the reduction process was enhanced and the final pH stabilized at 6.8. The sediments examined by Yu (1991) were not impacted by a coal pile, but this demonstrates the profound influence flooded conditions can have on pH.

2.3 Objective and Scope

The objective of this study was to measure two geochemical parameters, site-specific desorption K_d values and the Potentially Leachable Fraction, for contaminants from a D-Area Coal Pile Runoff Basin (DCPRB) sediment. The Potentially Leachable Fraction is a construct design to identify the fraction of a contaminant that is more readily available for leaching into water. The potential leachable fraction is analogous to the “Available Fraction” in a related work (Powell et al. 2004), although each of these constructs is operationally defined based on a different set of desorption (leaching) experiments. It is operationally defined by a set of selective extractions, with the intent of providing a conservative (high) estimate of the percentage of a contaminant that may leach from the sediment. The contaminant pool not associated with the Potentially Leachable Fraction can only be extracted from the sediment with extremely strong acids and reductants that dissolve minerals. The magnitude of the Potentially Leachable Fraction is expected to depend on the sorption mechanism of the contaminant to the sediment. In addition to quantifying these geochemical input values, these experiments were also designed to provide

---

[2] $½MnO_2 +2H^+ + e^- = ½Mn^{2±} + H_2O$
$Fe(OH)_3 + 3H^+ + e^- = Fe^{2+} + H_2O$
$1/8SO_4^{2-}\ 5/4H^+ + e^- = 1/8H_2S + 1/2H_2O$

the technical justification needed to use these constructs to describe the natural attenuation occurring at the site.

Particular attention was directed at evaluating the influence of flooded and non-flooded conditions on contaminant retention. As mentioned in the Introduction, variations in sediment moisture status induce profound geochemical changes that can influence contaminant sorption.

Experiments were conducted with a sediment collected from the basin floor of the DCPRB. The constituents evaluated were As, Be, Cd, Co, Cr, Cu, Ni, Pb, Sb, Se, Tl, and V. They include some groundwater constituents of concern (As, Be, and Ni), constituents that existed in high concentrations in the sediment (Cd, Co, Pb, Sb, Se, and Tl), and constituents that were among early suspects of constituents of concern (Cr, Cu, and V). Finally, due to budget constraints, only constituents that could be detected by inductively couple plasma – atomic emission spectroscopy (ICP-AES) were evaluated.

3.0 Materials and Methods

3.1 Materials

The sediment used in this study was collected from an exposed portion of the DCPRB bottom. The sample was collected on 17August02 by Kim Powell and Dan Kaplan (SRTC) with a shovel and placed in polyethylene bags. Prior to collecting the 15-cm deep surface sample, any large surface organic matter (leaves and sticks) was removed. The samples were stored at 4 °C in a field moist state. The sample was highly stratified in terms of texture and color. Chemical characterization was conducted on the sediment while it was in the moistened state to reduce artifacts imposed by the drying process, such as elevating pH, organic matter concentrations, and lowering crystalline Fe-oxide concentrations (Bartlett and James 1980). Standard methods were used to characterize the sediments (Sparks 1996):

- pH by the 1:1 sediment water slurry method,
- organic matter by the dry combustion method,
- particle size distribution by the sieving and pipette method,
- surface area by the N_2-gas adsorption method,
- amorphous Fe-oxide content by the 4-hr ammonium oxalate extraction method,
- crystalline Fe-oxide content by the dithionite-citrate-bicarbonate extraction method,
- cation-exchange capacity by the unbuffered salt (0.2 *M* ammonium chloride) extraction method, and
- anion-exchange capacity by the unbuffered salt (0.2 *M* ammonium chloride) extraction method.

An uncontaminated surface water was collected from Upper Three Runs Creek on 29August02 by Dan Kaplan and stored at 4 °C. The surface water sample was analyzed by standard methods for metals, anions, organic carbon, inorganic carbon, and pH.

3.2 Methods

Approximately 100 g of Runoff Basin sediment and 650 mL of uncontaminated SRS surface water were placed in each of two glass reaction vessels (Figure 2). The sediment slurries were maintained at 30 °C (to optimize for microbial activity) and under an Ar environment for 80 days. During this time, a small fraction of the aqueous phase (<0.1%) was slowly pumped from the reaction vessel, past a series of in-line sensors (pH, Eh, O_2, NH^+, and electrical conductivity) and then returned back to the reaction vessel through a low volume (1.4 mL), gas-impermeable tubing. ICP-AES analyses were conducted on acidified samples periodically collected from the reaction vessel. Ion Chromatography (IC) was conducted on non acidified split samples. In-line measurements were terminated after 17 days because of clogging of the fine tubing, after which time, the same measurements were made in traditional batch mode in the laboratory. Throughout the study, efforts were made to minimize air contact with the reaction vessel and aqueous samples. After 36 days, molasses was added to the reaction vessels to stimulate microbial activity. This was done because the system had appeared to reach a steady state and the introduction of a carbon source would promote microbial activity and an electron source to further reduce the system.

All electrode measurements were made in pure aqueous systems or with minimal contact with the sediment to minimize liquid junction potential error (Jenny et al., 1950). Eh measurements were made with a silver chloride/KCl electrode. To correct reported values to standard hydrogen electrode (SHE) values, add 0.210 V.

Immediately after the 80-day incubation period, the sediments were recovered and subjected to a five-step sequential extraction procedure (modified method of Hall et al., 1995; Miller et al. 1986). Details of this procedure are presented in Kaplan and Serkiz (2001). Briefly, 0.5 g samples of the treated sediments were extracted by a series of solutions that targeted operationally defined contaminant fractions. The extracts were increasingly aggressive at removing contaminants. The five fractions were: 1) extractable (1.0*M* CH_3COONa, pH 5); 2) amorphous Fe-oxide [0.25*M* $(NH_4)_2OH{\cdot}HCl$ in 0.25*M* HCl at 60°C for 30 min]; 3) crystalline Fe-oxide [1.0*M* $(NH_4)_2OH{\cdot}HCl$ in 25% CH_3COOH at 90°C for 3 hr]; 4) organic/sulfide (30% H_2O_2 pH 2 at 80°C for 2 hr); and 5) residual (total microwave digestion in 0.6 g solid + 10 mL HNO_3 + 4 mL H_2SO_4 + 2 mL HCl). The resulting extract solutions were acidified for sample preservation and characterized by ICP-AES. Between each extraction, the sediment was washed for 30 min with 0.01 *M* $CaCl_2$.

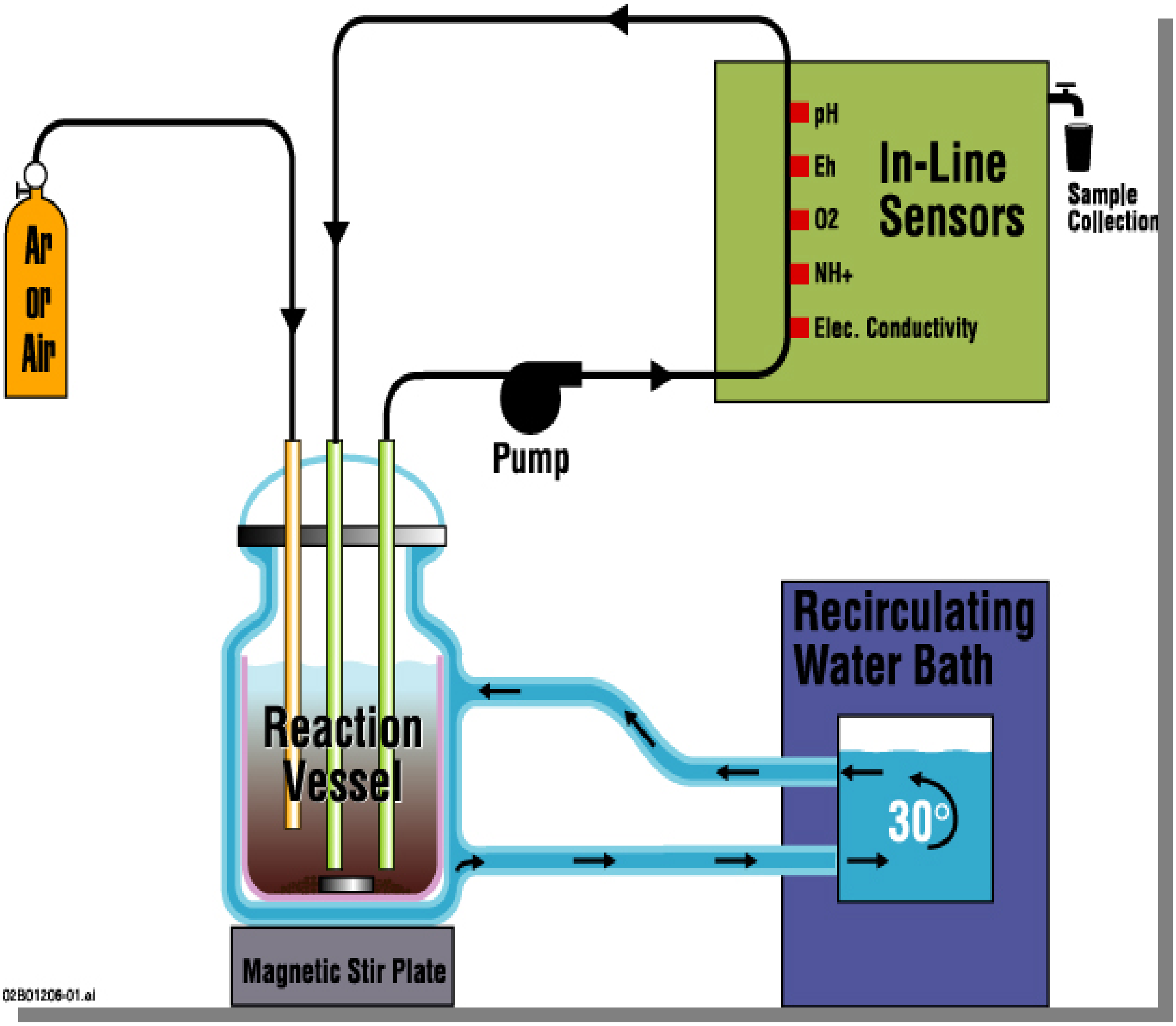

Figure 2. Experimental set up showing the reaction vessel containing an SRS surface water and the D-Area Coal Pile Runoff Basin sediment. The reaction vessel was maintained at 30 °C with a recirculating water bath and in an Ar (reducing) atmosphere. Water chemistry was monitored through the use of in-line sensors (sampled from a 1.4-mL sample loop) and periodic sample collections.

4.0 Results

The uncontaminated surface water used in this study was typical of such water found on the SRS (Table 1). It was acidic (pH 5.6) had low solute concentrations, and very low or undetectable contaminant concentrations. The DCPRB sediment was very acidic (pH 3.6) (Table 2). Its cation- and anion-exchange capacities are somewhat higher than many SRS sediments and may be the result of its unexpectedly high organic matter concentration (3.2 %). Its high surface area can be attributed to its sandy loam texture (fine texture) and high Fe oxide content. The sediment has As, Cd, Co, Sb, Se, and Tl concentrations that are more than two times background levels (Table 3). Be, Cr, Cu, Ni, and V concentrations were less than two times background levels.

Photographs of the sediment maintained under oxygenated (air sparged) and reducing (Ar sparged) conditions for 80-days is presented in Figure 3. The reduced sediment is much darker than the oxidized sediment, consistent with sediment color changes observed in nature, and is indicative of significant chemical and mineralogical changes. The grayish color of reduced sediments is likely attributed to the formation of iron sulfides and hydrate magnetite ($Fe_3O_4 \cdot nH_2O$ or $Fe_3(OH)_8$) along with some hydrotrolite ($FeS \cdot nH_2O$). If anaerobic conditions persist and chemical conditions are favorable, these precipitates may age, producing the typical minerals of reduced sediment, magnetite (Fe_3O_4), and pyrite (FeS_2) (Schmertmann and Taylor 1989. Also Fe(II) silicates (greenalite and chamosite), and vivianite ($Fe_3(PO_4)_2 \cdot 8H_2O$) have been reported in submerged sediments (Schmertmann and Taylor 1989).

4.1 Aqueous Chemistry as a Function of Redox Conditions

During the 80-day trial, the primary water chemistry indicators, pH, Eh (a measure of redox potential) and electrical conductivity (a measure of total salts in solution) followed well established trends (Figure 4; additional data is presented in Appendix A; Ponnamperuma 1972). Eh decreased as time elapsed after adding water to the sediment. As Eh decreases, pH generally increased in response to a number of chemical reactions, including the dissolution of Fe/Mn/Al-oxyhydroxides causing the release of OH^- into solution. The initial decrease in pH shortly after submergence is commonly observed and has been attributed to the accumulation of CO_2 produced by respiration of aerobic bacteria. Ponnamperuma et al. (1969) reported that the pH of most submerged sediments equilibrated with CO_2 at 1 atm is 6.1. Changes in electrical conductivity occurred in ways that have been previously observed in other sediments (Ponnamperuma 1972). Typically the specific conductance of the solutions increases after submergence, attains a maximum, and declines to a fairly stable value, which varies with the sediment. The changes in conductance reflect the balance between reactions that produce ions and those that inactivate them or replace them with slower moving ions. The general increase in electrical conductivity can be attributed to the dissolution of Fe/Al/Mn-oxyhydroxides and the release of cations and anions sorbed to these strong sorbents (discussed in more detail below). Once molasses was added at day 36, the redox dropped significantly from about 0.200 to 0.000 V (or 0.410 to 0.210 V versus standard hydrogen electrode) in the control . Importantly, the redox status of the system did not significantly decrease until it was biostimulated with the molasses. Electrical conductivity increased largely in response to the introduction of charged soluble species in the molasses.

The concentrations of the naturally occurring constituents that are redox sensitive (O_2, NO_3^-, Mn, Fe, and SO_4^{2-}) changed in the well defined manner defined in Eq. 3 (Figure 5, Figure 6, and Figure 7). Theoretically, as a system becomes increasingly reduced due to flooding, $O_2(aq)$ reduces to H_2O and then NO_3^- reduces to NH_4^+. Then Mn(III/IV) minerals dissolve, followed by Fe(III) minerals. Finally sulfide minerals are formed. Once water was added to the sediment, O_2 and then NO_3^- concentrations decreased quickly. Fe and Mn concentrations started increasing essentially immediately, likely the result of these oxyhydroxides dissolving in response to the lowering redox status (or to the conversion of sorbed Fe^{3+} reducing to Fe^{2+} and desorbing from the sediment). Sulfate concentrations also increased prior to the molasses addition, likely being released during Fe-oxyhydroxide dissolution and to the increased pH, which made the anion-exchange capacity of the sediment decrease. Most sulfate in coastal plain sediments are associated with Fe-oxyhydroxides, and once the Fe-oxyhydroxides started to undergo reductive dissolution, but before sulfate reduction, sulfate was released into the aqueous phase. Once molasses was added (Figure 6), sulfate, a constituent of molasses, concentrations initially increased, but shortly afterwards gradually declined, likely the result of sulfate reduction (which precedes appreciably faster in higher pH environments). Nitrate concentration also initially increased after the molasses addition, but then re-equilibrated at about the same concentrations as existed prior to the molasses addition. Fe concentration steadily increased through out the study, likely the result of various Fe-phases solubilizing as the Eh decreased (Figure 7). By the end of the 80-day trial, Fe concentrations had increased 40 times greater than its original concentration under oxidized conditions.

Table 1. Chemical composition of the SRS uncontaminated surface water.

Constituent	Units	Concentration	Method
pH		5.6	pH meter
TIC	ppm	0.713	O.I. Corp Total Organic C
TOC	ppm	0.514	O.I. Corp Total Organic C
Ag, Al, As, Be, Cd, Co, Cr, Fe, K, Mn, Mo, Ni, P, Pb, Sb, Se, Ti, U, Zn	ppm	BDL	ICP-AES
B	ppm	0.147	ICP-AES
Ba	ppm	0.003	ICP-AES
Ca	ppm	0.402	ICP-AES
Cu	ppm	0.003	ICP-AES
Mg	ppm	0.287	ICP-AES
Si	ppm	3.023	ICP-AES
Sr	ppm	0.003	ICP-AES
Li	ppb	0.209	ICP-MS
Na	ppb	154.2	ICP-MS
K	ppb	182.7	ICP-MS
Mn	ppb	1.653	ICP-MS
Fe	ppb	0.055	ICP-MS
Be, Cd	ppb	BDL	ICP-MS
Al	ppb	1.393	ICP-MS
Cr	ppb	0.005	ICP-MS
Co	ppb	0.167	ICP-MS
Ni	ppb	0.468	ICP-MS
Zn	ppb	3.131	ICP-MS
Cu	ppb	18.602	ICP-MS
As	ppb	0.081	ICP-MS
Sr	ppb	4.289	ICP-MS
Mo	ppb	0.759	ICP-MS
Ag	ppb	0.104	ICP-MS
Sn	ppb	0.189	ICP-MS
Ba	ppb	8.166	ICP-MS
Pb	ppb	1.312	ICP-MS
Cl^-	ppm	2.678	Bran-Lubbe Wet Chemistry
NH_4^+	ppm	0	Bran-Lubbe Wet Chemistry
PO_4^{3-}	ppm	<0.001	Bran-Lubbe Wet Chemistry
Total P	ppm	0	Bran-Lubbe Wet Chemistry
$NO_3 + NO_2$	ppm	0.832	Bran-Lubbe Wet Chemistry
Total N	ppm	0.795	Bran-Lubbe Wet Chemistry
NO_2	ppm	0	Bran-Lubbe Wet Chemistry
SO_4^{2-}	ppm	<0.556	Bran-Lubbe Wet Chemistry

Table 2. Characterization of sediment collected from the D-Area Coal Pile Runoff Basin.

Analyte	Avg ± Stdev (2 reps)	Method[a]
pH	3.59 ± 0.01	1:1 sediment water slurry
Organic Matter (wt-%)	3.2 ± 0.1	Dry combustion
Sand/Silt/Clay (wt-%)	63/29/8	Sieving and pipette
Surface Area (m^2/g)	17.5	N_2-gas adsorption
Amorphous Fe-oxide (wt-%)	0.23 ± 0.02	4-hr ammonium oxalate in the dark
Crystalline Fe-oxide (wt-%)	1.18 ± 0.11	Dithionite-citrate-bicarbonate
Cation Exchange Capacity ($cmol_{(+)}/kg$)	2.21 ± 0.38	0.2 *M* NH_4Cl exchange
Anion Exchange Capacity ($cmol_{(-)}/kg$)	0.54 ± 0.28	0.2 *M* NH_4Cl exchange

[a] Sparks, 1996.

Table 3. Contamination concentrations in Runoff Basin sediment vs. background levels.

	Runoff Basin Rep. 1	Runoff Basin Rep. 2	Runoff Basin Avg.	Background[a]	Is Runoff Basin Sample >2x Background?
As	277.8	191.3	234.6	0.6	Yes
Be	0.3	0.8	0.5	0.7	No
Cd	5.7	4.2	5.0	0.2	Yes
Co	3.8	1.3	2.5	1.0	Yes
Cr	10.1	9.2	9.7	8.1	No
Cu	0.5	1.1	0.8	12.4	No
Ni	8.1	3.3	5.7	4.1	No
Pb	59.1	26.2	42.6	10.6	Yes
Sb	60.2	25.5	42.9	<10.6[b]	Yes
Se	147.2	76.8	112.0	<0.4[b]	Yes
Tl	108.7	19.1	63.9	0.1	Yes
V	22.9	26.9	24.9	13.5	No

[a] Background from WSRC-RP-99-4067, Rev. 0, Arithmetic Mean of 3 sites (RCRA Facility Investigation/Remediation Investigation Work Plan Addendum for the D-Area Expanded Operable Unit (U)

[b] Average of site wide survey of surface soils and sediments (Table 6.1 in Looney et al. 1990).

Figure 3. D-Area Coal Pile Runoff Basin sediment under oxidized conditions (on the right in both photographs) and reduced conditions (on the left in both photographs).

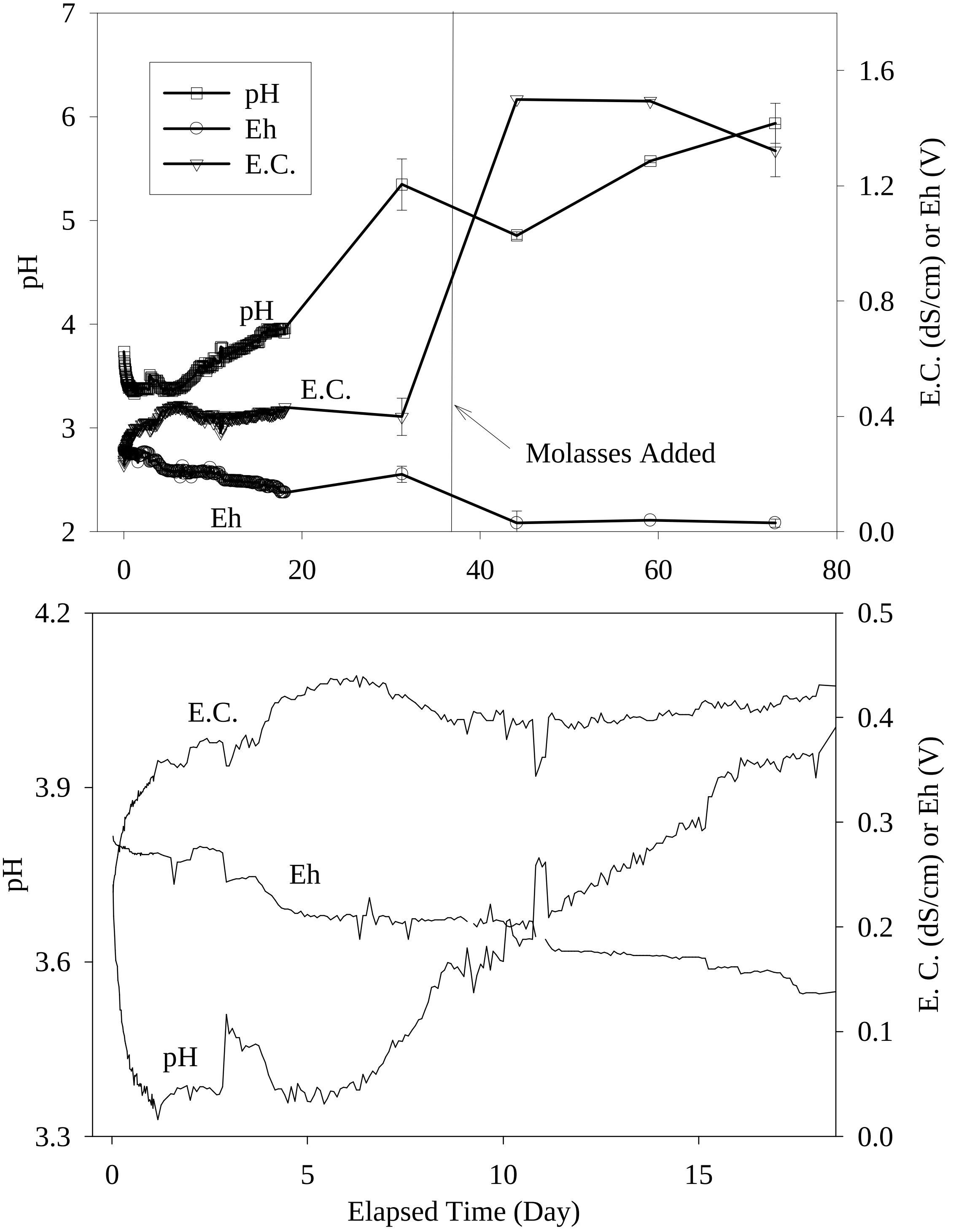

Figure 4. Porewater pH, electrical conductivity (E.C.), and reduction potential (Eh; reported versus silver:silver chloride; to correct to standard hydrogen electrode add 0.210 V to reported values) as a function of time after flooding the Seepage Basin sediment (Top: full data set; Bottom: data from 0 to 18 days).

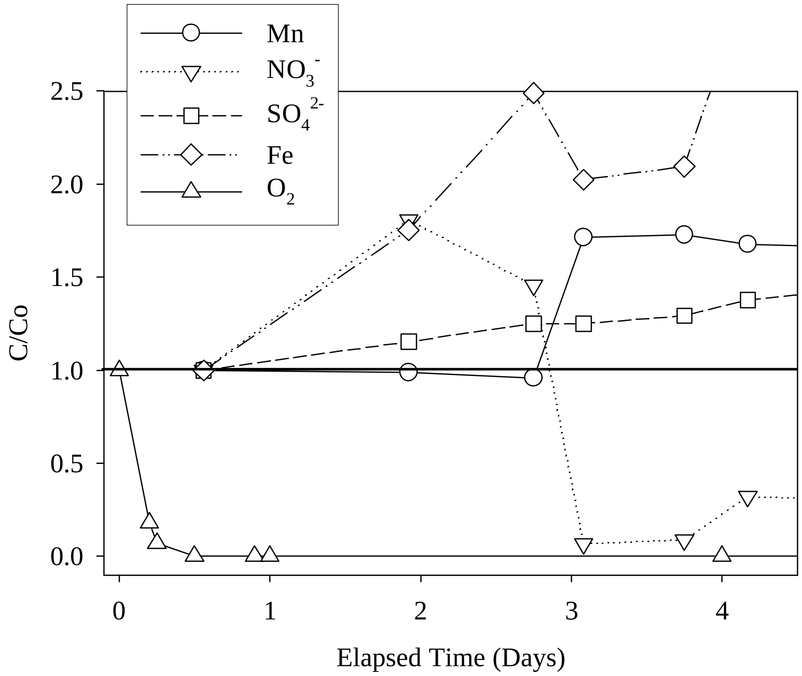

Figure 5. Porewater concentrations of redox-sensitive constituents during the first 4 days after flooding (C/Co is the solute concentration normalized to its concentration at time zero).

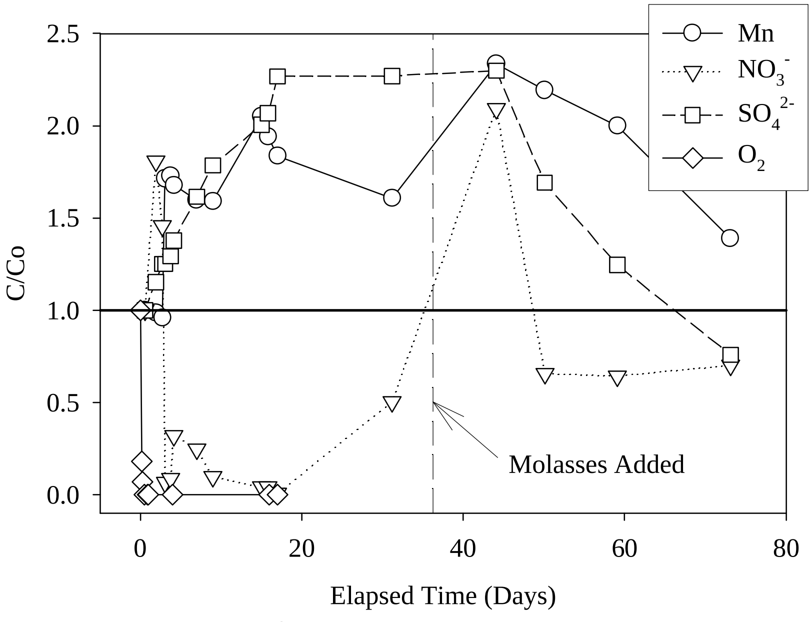

Figure 6. Porewater concentrations of redox-sensitive constituents vs. elapsed time after flooding (C/Co is the solute concentration normalized to its concentration at time zero. Molasses added 36 days after initiating flooded conditions).

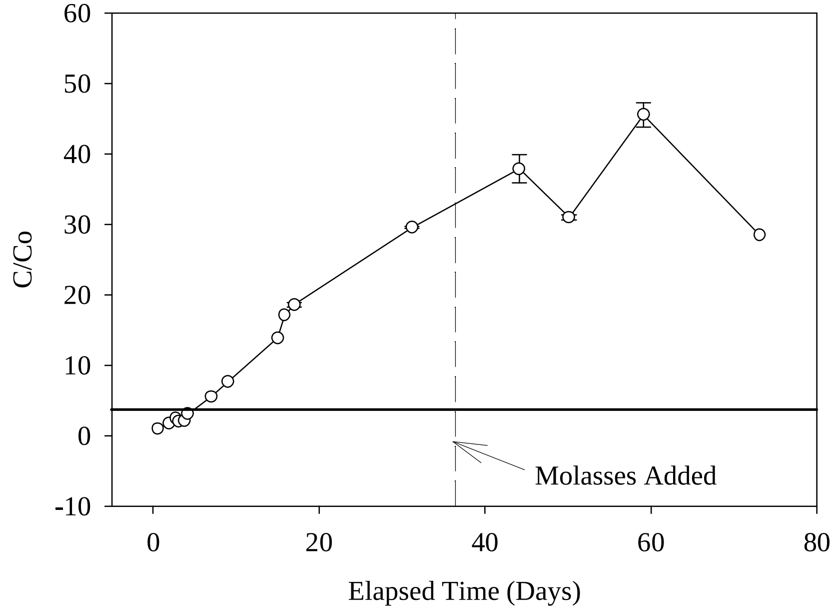

Figure 7. Porewater Fe concentrations vs. elapsed time after flooding (C/Co is Fe concentrations normalized to its concentration at time zero. Molasses added 36 days after initiating flooded conditions).

Changes in aqueous contaminant concentrations during the entire experiment can be classified in four categories (Figure 8, Figure 9, and Figure 10):

- no systematic change: As and Se,
- no change until molasses was added and then the contaminant concentrations significantly ($p \leq 0.05$) decreased: Cd, Co, Cr, Ni and Tl,
- at first, contaminant concentrations gradually increased and then once molasses was added, the contaminant concentrations significantly ($p \leq 0.05$) decreased: Cu and V,
- most of the data was below the detection limit: Be.

It is important to note that simply by placing this source term sediment under reducing conditions, i.e., flooding the site, aqueous contaminant concentration did not decrease without biostimulation. In fact, in the third category above, sediment Cu and V decreased after flooding and biostimulation, presumably the result of dissolving the sorbing Fe-oxyhydroxides in the sediment (Figure 7). After biostimulation, almost all contaminant concentrations, except As, Se, and Be, decreased.

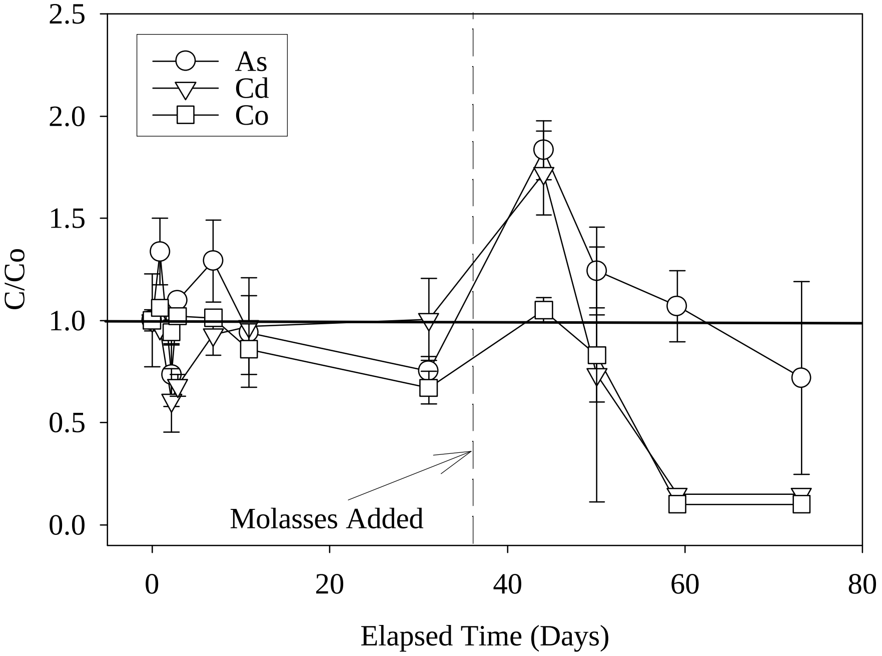

Figure 8. As, Cd, and Co porewater concentrations vs. elapsed time after flooding (C/Co is the solute concentration normalized to its concentration at time zero. Molasses added 36 days after initiating flooded conditions).

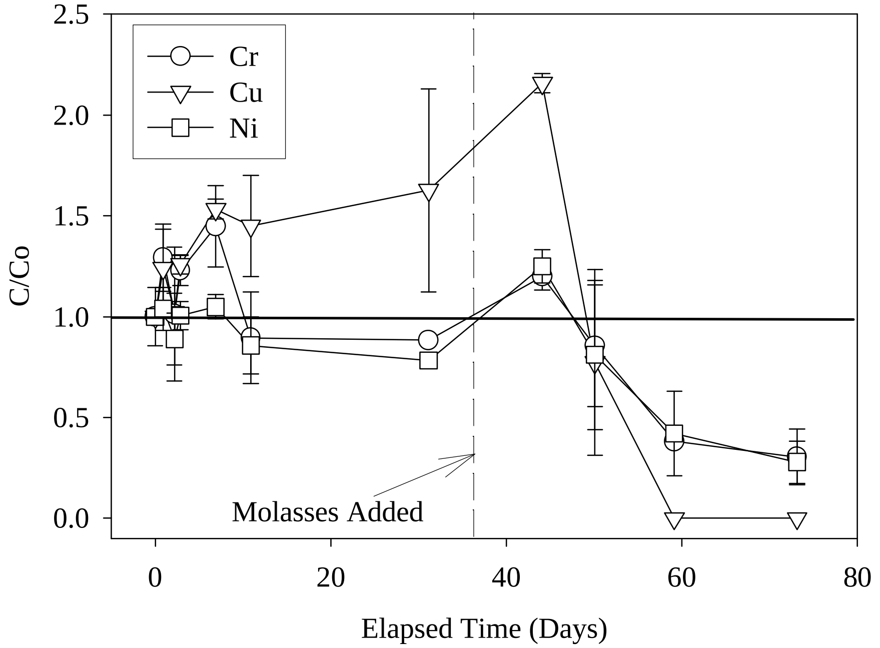

Figure 9. Cr, Cu, and Ni porewater concentrations vs. elapsed time after flooding (C/Co is the solute concentration normalized to its concentration at time zero. Molasses added 36 days after initiating flooded conditions).

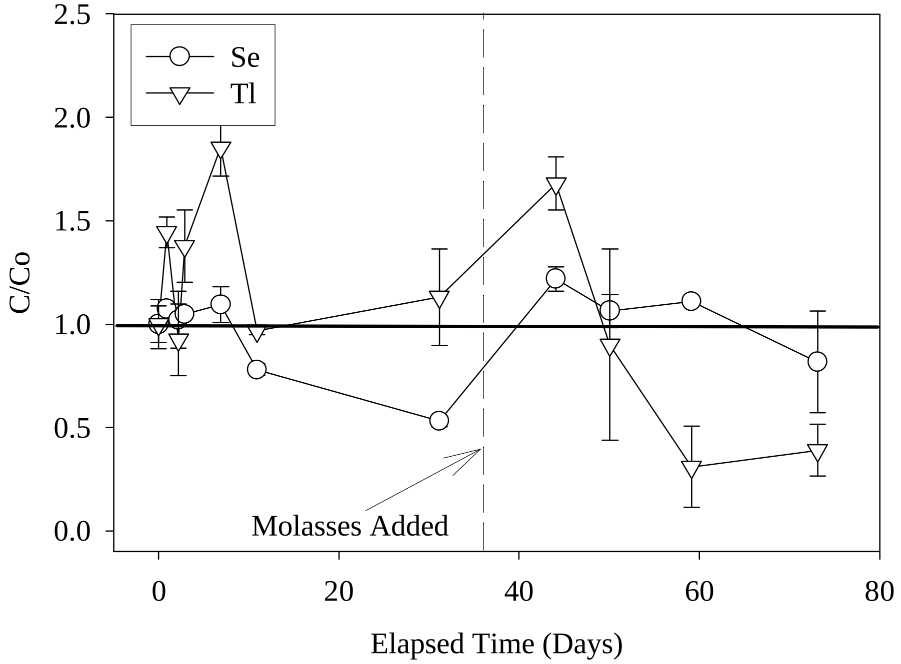

Figure 10. Se and Tl porewater concentrations vs. elapsed time after flooding (C/Co is the solute concentration normalized to its concentration at time zero. Molasses added 36 days after initiating flooded conditions).

4.2 Source Term K_d Values as a Function of Redox Condition

Desorption K_d values, the ratio of the contaminant concentration on the solids divided by the contaminant concentrations in the aqueous phase, were calculated using Eq. 5, sequential extraction data (detailed data presented in Appendix A), and the aqueous data presented in Figure 8, Figure 9 and Figure 10 .

$$K_d = \frac{C_{Exch} + C_{AmorphFe} + C_{Org}}{C_{aq\ t=x}} \qquad (5)$$

where:

C_{Exch} = contaminant concentration associated with the exchangeable sequential extraction fraction (μg/g),
$C_{AmorphFe}$ = contaminant concentration associated with the amorphous Fe-oxide sequential extraction fraction (μg/g),
C_{Org} = contaminant concentration associated with the organic sequential extraction fraction (μg/g), and

$C_{aq\ t=x}$ = contaminant porewater concentration at time x, where x is 0, 31, or 80 days (µg/mL).

Three K_d values were calculated: $K_{d\text{-Oxidized}}$, $K_{d\text{-Reduced}}$, and $K_{d\text{-BioReduced}}$. $K_{d\text{-Oxidized}}$ values were determined under conditions that approximated present, unsaturated, oxidizing conditions Table 4. The aqueous contaminant concentrations, the denominators, used in the K_d calculations were those measured one day after flooding. $K_{d\text{-Reduced}}$ values were determined under conditions that approximated natural reducing conditions without biostimulation. The aqueous contaminant concentrations used in the $K_{d\text{-Reduced}}$ calculations were those measured 31 day after flooding, the last measurement prior to biostimulation with molasses. $K_{d\text{-BioReduced}}$ values were determined under conditions that had undergone biostimulation through the addition of molasses as an electron and carbon source.

The operational definition of these K_d values are quite similar to the *in situ* K_d values described by Powell et al. (2004) in a related report. They defined C_{solid} (Eq. 1) as being equal to the Available Fraction (defined by several early extraction steps in their sequential extraction method; the Available Fraction is near identical to the %-Leachable Fraction defined in Eq. 6). C_{liquid} (Eq. 1) was defined by Powell et al. (2004) as the constituent of concern concentration in the sediment pore water naturally existing in the sample at the time of sampling. As such, it is quite similar to the desorption K_d value measured for this report.

Table 4. K_d values of contaminants in a sediment flooded for 1 day ($K_{d\text{-Oxidized}}$), a sediment flooded for 31 days ($K_{d\text{-Reduced}}$), and in a sediment flooded for 36 days & biostimulated for 44 days ($K_{d\text{-BioReduced}}$).[a]

	$K_{d\text{-Oxidized}}$ (mL/g)		$K_{d\text{-Reduced}}$ (mL/g)		$K_{d\text{-BioReduced}}$(mL/g)	
Element	Avg.	Stdev.	Avg.	Stdev.	Avg.	Stdev.
As	295	28	834	35	1065	698
Be[b]	>526	NA	356	146	>551	NA
Cd	67	32	163	44	>168	NA
Co	41	30	126	6	>180	NA
Cr	110	51	431	160	1784	814
Cu	22	4	352	48	>691	NA
Ni	64	52	178	16	563	212
Se	83	79	209	18	146	44
Tl	79	80	252	30	808	259
V	2514	627	861	92	1702	443
Al	2374	414	8320	2873	29588	17377
Fe	92	29	162	122	65	27
Mn	5	6	13	1	19	5

[a] K_d values were calculated using Eq. 5. $K_{d\text{-Oxidized}}$ values were determined under conditions that approximated present, as is, conditions. $K_{d\text{-Reduced}}$ values were determined under conditions that approximated natural reducing conditions without biostimulation. $K_{d\text{-BioReduced}}$ values were determined under conditions that had undergone biostimulation, i.e., addition of molasses. Sediment used to estimate the $K_{d\text{-BioReduced}}$ were flooded for 36 days, amended with molasses, and then left to equilibrate for an additional 44 days.

[b] Be K_d values are suspect because many of the sediment and porewater analytical values used in the calculations were near or below detection limit.

The change in K_d values during the 80-day trial followed four general trends (Table 4):

- K_d values increased during the study: As, Cd, Co, Cr, Cu, Ni, and Tl,
- K_d values had a maximum just prior to biostimulation: Se,
- K_d values decreased after flooding and slightly increased after biostimulation: V, and
- K_d values could not be reliably measure due to low contaminant concentrations: Be.

Thus, in general, the sediment's ability to hold contaminants increased as the redox decreased, except for Se and V. This is consistent with the general notion that many contaminants are more strongly bound to sediments under reducing conditions.

4.3 Potentially Leachable Fraction

An index of the contaminant fraction that has the potential of entering into the mobile aqueous phase was estimated using Eq. 6:

$$\text{Potentially Leachable Fraction} = 100 - (F_{\text{CrystFe}} + F_{\text{Residual}}) \qquad (6)$$

where:

F_{CrystFe} = crystalline Fe-oxide sequential extraction fraction (wt-%), and
F_{Residual} = residual sequential extraction fraction (wt-%).

The idea behind this construct is that the entire contaminant pool may not be assessable to the mobile aqueous phase. Some fraction of the contaminant pool may be very strongly bound by the sediment, for example, that fraction covalently bound within mineral structures. Thus, the Potentially Leachable Fraction is an estimate of that portion of the contaminant pool that can likely enter the mobile aqueous phase. It excludes the contaminant fraction held within crystalline Fe-oxyhydroxides and other chemically resistant sediment minerals, such as silicates and aluminosilicates.

The Potentially Leachable Fraction varied between 14 and 100% (Table 5). Under oxidized conditions, the Potentially Leachable Fraction was:

<33% for As, Cd, Se, and V,
>33% but <66% for Be, Co, Cr, and Ni,
>67% for Cu and Tl.

This indicates that based on this estimate that less than a third of the As, Cd, Se, and V in the DCPRB sediment is likely to enter the aqueous phase. Conversely, most of the Cu and all the Tl may be expected to enter the aqueous phase.

Under more reducing conditions, the Potentially Leachable Fraction increased or remained the same, but never decreased (Table 5). Thus, we have seemingly contradictory results in that the Kd values indicated that sorption generally increased after flooding and biostimulation, whereas the Potentially Leachable Fraction data suggested the opposite occurred. Apparently, most of the increased sorption of contaminants that occurred under reducing conditions, as measured by the K_d values, occurred in weakly binding sites, i.e., the exchangeable, amorphous Fe-oxide or the organic/sulfide sites. The total amount of contaminant on the sediment increased under reducing conditions, but this newly sorbed fraction tended to accumulate in the weakly binding sites.

Table 5. Potentially Leachable Fraction (wt-%) under oxidized and reducing conditions.[a]

Element	Oxidized Conditions		Reduced Conditions	
	Avg	Stdev	Avg	Stdev
As	14	13	27*	0
Be	54	17	70	0
Cd	25	7	47*	7
Co	67	5	73	2
Cr	45	23	73*	1
Cu	86	20	100	0
Ni	46	18	76*	1
Se	19	12	36*	2
Tl	100	0	100	0
V	30	0	53*	1
Al	15	0	27*	2
Fe	16	0	23*	3
Mn	28	3	86*	6

[a] Potentially leachable fraction is defined in Eq. 5. Oxidized Conditions values were measured from a field-moist sediment sample. Reduced Condition values were measured in the sediment recovered from the 80-day flooding/biostimulation experiment.

* Identify means within a row that are significantly greater ($p \leq 0.05$, $n = 2$), according to Student's two-tailed *t*-test.

5.0 References

Bartlett, R., and B. James. 1990. Studying Dried, Stored Soil Samples – Some Pitfalls. *Soil Sci. Soc. Am J.,* 44:721-724.

Bouwer, H. 1991. Simple Derivation of the Retardation Equation and Application to Preferential Flow and Macrodispersion. *Ground Water*, 29: 41–46.

Clark, S. B., W. H. Johnson, M. A. Malek, S. M. Serkiz, T. G. Hinton. 1996. *Radiochim. Acta,* 74: 173–178.

Hall, G. E. M., J. E. Vaive, R. Beer, M. Hoashi. 1996. Selective Leaches Revisited, with Emphasis on the Amorphous Fe Oxyhydroxide Phase Extraction. *J. Geochem. Exploration,* 56: 59–78.

Jenne, H., T. R. Nielsen, N. T. Coleman, and D. E. Williams. 1950. Influence of Iron Reduction of Sediments on Analyte Availability. *Science,* 112:164–167.

Kaplan, D. I., and S. M. Serkiz. 2000. *In-situ Kd Values and Geochemical Behavior for Inorganic and Organic Constituents of Concern at the TNX Outfall Delta*. WSRC-TR-99-00488. Westinghouse Savannah River Company, Aiken, SC.

Kaplan, D. I., and S. M. Serkiz. 2001. Quantification of Thorium and Uranium Sorption to Contaminated Sediments. *J. Radioanalytical NuclearChem.* 248(3): 529–535.

Krupka, K. M., D. I. Kaplan, G. Whelan, R. J. Serne, and S. V. Mattigod. 1999. *Understanding Variation in Partition Coefficient, Kd, Values. Volume II: Review of Geochemistry and Available Kd Values, for Cadmium, Cesium, Chromium, Lead, Plutonium, Radon, Strontium, Thorium, Tritium (^{3}H), and Uranium.* EPA 402-R-99-004A. Office of Air and Radiation, Office of Solid Waste and Emergency Response, U.S. Environmental Protection Agency, Washington, DC. (http://www.epa.gov/radiation/cleanup/partition.htm)

Looney, B. B., C. A. Eddy, M. Ramdeen, J. Pickett, V. Rogers, M. T. Scott, and P. A. Shirley. 1990. *Geochemical and Physical Properties of Soils and Shallow Sediments at the Savannah River Site*. WSRC-RP-90-1031. Westinghouse Savannah River Site, Aiken, SC.

Miller, W. P., D. C. Martens, and L. W. Zelazny. 1986. Forms of Solid Phase Copper in Copper-Enriched Swine Manure. *Soil Sci. Soc. Am. J.,* 50:598–601.

Moore, R. M., and G. E. Millward. 1984. Dissolved-Particulate Interactions of Aluminum in Ocean Waters. Geochim. Cosmochim. Acta, 48(2): 235-241.

Nirel, P. M. V., and F. M. M. Morel. 1990. Pitfalls of Sequential Extractions. *Wat. Res.*, 24: 1055–1056.

Nyffeler, U. P., Y. H. Li, P. H. Santschi. 1984. A Kinetic Approach to Describe Trace Element Distribution Between Particles and Solution in Natural Aquatic Systems. Geochim. Cosmochim. Acta, 48(7): 1513–1522.

Ponnamperuma, F. N. 1972. The Chemistry of Submerged Soils. *Adv. Agron.,* 24:29–96.

Ponnamperuma, F. N., R. U. Catro, and C. M. Valencia. 1969. *Soil Sci. Soc. Amer. Proc.*, 33: 239–241.

Powell, K. R., S. Serkiz, A. Pishko, P. C. McKinsey, R. L. Brigmon, E. P. Shine, C. Fliermans, and A. S. Knox. 2004. *Monitored Natural Attenuation of Inorganic Contaminants Treatability Study Final Report.* WSRC-TR-2004-124, Rev. 0., Westinghouse Savannah River Company, Aiken, SC.

Schwertmann, U., and R. M. Taylor. 1989. Iron Oxides. pp. 379–438. In: Dixon, J. B., and S. B. Week (eds.), *Minerals in Soil Environments, 2nd Edition*, Soil Science Society of America, Madison, WI.

Serne, R. J., and V. L. LeGore. 1996. *Strontium-90 Adsorption-Desorption Properties and Sediment Characterization at the 100 N-Area*. PNL-7145, Pacific Northwest National Laboratory, Richland, WA.

Sparks, D. L. 1996. *Methods of Soil Analysis, Part 3 – Chemical Methods.* Soil Science Society of America, Madison, WI.

Specht, W. L. 1999. *Results of Toxicity Tests and Chemical Analyses Conducted on Sediments Collected from the TNX Outfall Delta Operable Unit.* WSRC-TR-99-00380. Westinghouse Savannah River Company, Aiken, SC.

Sposito, G. 1986. *The Chemistry of Soils.* Oxford University Press, New York.

Stumm, W., and J. J. Morgan. 1996. *Aquatic Chemistry.* 3rd Edition. Wiley-Interscience Publishers, NY.

Tessier, A., P. G. C. Campbell, and M. Bisson. 1979. Sequential Extraction Procedure for the Speciation of Particulate Trace Metals. *Analyt. Chem.* 51: 844–851.

Turner, F. T., and W. H. Patrick. 1968. Chemical Changes in Waterlogged Soils as a Result of Oxygen Depletion. *Trans. IX Congress, International Soil Science Society,* 4:53-65.

Valocchi, A. J. 1984. Describing the Transport of Ion-Exchanging Contaminants Using an Effective K_d Approach. *Water Resour. Res.*, 20(4): 499-503.

Veizer, J. 1983. Trace Elements and Isotopes in Sedimentary Carbonates. pp. 265–300. In: *Carbonates: Mineralogy and Chemistry,* R. J. Reeder (ed.). Mineralogical Society of America, Blacksburg, VI, Yu, T. R. 1991. Characteristics of Soil Acidity of Paddy Soils in Relation to Rice Growth. pp. 107-112. In: *Plant-soil Interactions at Low pH.* R. J. Wright et al. (eds.), Kluwer Academic Publishers, Netherlands.

6.0 Appendix A. Additional Data

Table A 1. Sequential extraction results for the untreated sediment (wt-%).

	Exchangeable		Amorphous Fe-oxide		Crystalline Fe-oxide		Organic/Sulfide		Residual	
	Avg	Stdev	Avg	Stdev	Avg	Stdev	Avg	Stdev	Avg	Stdev
Ag	20	5	59	24	21	29	0	0	0	0
Al	4	0	5	0	22	2	6	0	63	2
As	9	6	4	5	53	5	2	2	33	8
B	11	5	25	2	63	9	1	2	0	0
Ba	20	1	4	0	5	1	3	1	69	2
Be	27	19	25	2	46	17	2	0	0	0
Ca	44	1	37	4	2	2	0	1	17	5
Cd	9	2	17	5	72	4	0	0	3	4
Co	23	4	39	3	33	5	6	5	0	0
Cr	9	8	29	10	55	23	6	5	0	0
Cu	86	20	0	0	0	0	0	0	14	20
Fe	1	0	15	0	76	1	1	0	8	1
K	51	5	30	11	0	0	0	0	19	6
Mg	12	3	6	3	4	1	12	0	66	7
Mn	21	2	8	0	32	4	4	1	35	8
M	15	0	16	2	68	4	2	3	0	0
Na	100	0	0	0	0	0	0	0	0	0
Ni	21	8	22	5	15	6	3	4	40	24
P	2	2	6	2	72	3	2	1	18	2
Pb	8	11	19	5	28	10	2	4	43	29
Sb	11	8	14	6	72	18	3	4	0	0
Se	9	7	9	4	69	7	1	2	12	5
Si	8	2	14	0	51	3	26	1	1	0
Sr	7	0	4	0	1	0	3	1	85	1
Ti	2	1	2	0	1	0	26	3	69	1
Tl	17	24	83	24	0	0	0	0	0	0
V	2	1	25	1	70	0	3	1	0	0
Zn	13	0	11	0	23	0	4	0	50	0

Table A 2. Sequential extraction results for the treated (Ar gas/molasses addition) sediment (wt-%).

	Exchangeable		Amorphous Fe-oxide		Crystalline Fe-oxide		Organic/Sulfide		Residual	
	Avg	Stdev	Avg	Stdev	Avg	Stdev	Avg	Stdev	Avg	Stdev
Ag	29	9	53	23	16	28	2	2	0	0
Al	6	2	11	3	20	2	6	2	56	7
As	14	1	9	2	54	4	4	0	20	6
B	25	9	27	4	44	6	4	1	0	0
Ba	25	3	12	18	4	0	3	1	56	6
Be	23	12	38	16	37	12	3	2	0	0
Ca	75	3	14	7	2	0	0	0	9	0
Cd	19	5	22	1	53	5	5	1	1	2
Co	30	2	35	18	27	1	7	1	0	0
Cr	26	10	34	6	30	6	10	0	0	0
Cu	27	3	70	21	0	0	3	2	0	0
Fe	3	0	18	4	66	3	1	0	11	5
K	60	10	38	7	0	0	1	2	2	3
Mg	31	4	13	6	4	1	10	2	42	9
Mn	78	5	5	3	7	1	1	0	9	4
M	18	2	20	3	56	4	6	2	0	0
Na	100	0	0	13	0	0	0	0	0	0
Ni	30	5	34	17	24	1	7	1	5	9
P	6	1	26	10	53	2	4	1	11	5
Pb	20	4	26	7	37	2	5	2	12	10
Sb	19	1	20	11	55	2	7	2	0	0
Se	19	3	13	4	61	4	2	1	5	6
Si	18	3	24	10	38	4	20	4	1	1
Sr	22	3	9	4	1	0	3	1	65	5
Ti	6	2	10	3	4	1	26	8	54	14
Tl	41	2	55	28	0	0	4	3	0	0
V	7	2	40	15	49	3	5	1	0	0
Zn	54	23	22	9	3	0	1	0	20	18

Table A 3. Porewater chemistry in the Ar (reduced) treatment.

ID#	Time	pH	Eh	Cond	Al	As	Ba	Ca	Cd	Co
	(Days)		(V)	(dS/cm)	------------------------------- (ppm) -------------------------------					
206	0.6	3.405	0.269	0.318	2.291	0.0654	0.0737	7.799	0.0077	<0.003
207	1.9	3.362	0.264	0.371	2.552	0.0882	0.0662	8.18	0.0093	<0.003
208	2.8	3.385	0.271	0.376	2.667	0.0669	0.057	8.609	<0.003	<0.003
209	3.1	3.47	0.246	0.374	2.17	0.09	0.0751	10.44	0.0031	<0.003
210	3.8	3.44	0.24	0.389	2.367	0.0657	0.0798	11.1	0.0031	<0.003
211	4.2	3.382	0.221	0.414	2.842	0.0912	0.0762	11.85	0.0062	<0.003
212	7.0	3.446	0.21	0.423	<3.081	0.1131	0.0767	12.74	0.0031	0.0008
213	9.0	3.624	0.205	0.384	2.485	0.1077	0.0789	13.85	0.0031	<0.003
215	15.0	3.825	0.17	0.414	1.574	<0.1215	<0.0824	<15.93	<0.0139	0.0038
216	15.8	3.91	0.162	0.416	1.256	0.0969	0.0771	15.8	0.0124	0.0034
217	17.0	3.926	0.156	0.413	1.15	0.0816	0.0744	15.23	<0.0139	0.0015
455 & 456	31.2	5.345	0.160	0.249	0.273	0.068	<0.0824	13.755	0.02	0.027
467 & 468	44.1	4.855	0.030	1.500	0.243	0.166	<0.0824	22.71	0.035	0.043
471 & 472	50.1	5.035	0.040	1.500	0.10715	0.11225	<0.0824	21.36	0.0148	0.0337
475 & 476	59.1	5.570	0.040	1.494	0.067	0.097	<0.0824	20.255	<0.003	<0.003
479 & 480	73.1	5.935	0.030	1.322	0.077	0.065	<0.0824	15.065	<0.003	<0.003

Table A 4. Porewater chemistry in the Ar (reduced) treatment.

ID#	Time	Fe	K	Mg	Mn	Na	Ni	Si	Sr	NH_4^+	NO_3^- + NO_2^-	SO_4^{2-}
	(days)						(ppm)					
206	0.6	1.69	2.42	3.25	2.35	5.14	0.015	5.06	0.028	0.010	0.172	75.22
207	1.9	2.96	2.73	3.22	2.32	5.11	0.022	5.69	0.029	0.048	0.311	86.72
208	2.8	4.21	2.86	3.28	2.25	5.06	0.015	6.01	0.030	<0.114	<0.251	94.12
209	3.1	3.42	5.08	4.69	4.03	5.02	0.009	6.05	0.038	0.024	0.011	94.02
210	3.8	3.54	5.31	4.72	4.06	5.03	0.016	6.13	0.040	0.018	0.015	97.23
211	4.2	5.22	5.27	4.54	3.94	5.18	<0.063	6.65	0.042	0.040	0.055	103.64
212	7.0	9.35	6.79	4.37	3.75	5.20	0.024	8.11	0.045	0.038	0.042	121.45
213	9.0	12.94	7.75	4.39	3.74	5.38	0.023	9.17	0.049	0.067	0.016	134.24
215	15.0	23.45	11.33	<5.11	<4.82	5.62	0.039	10.39	<0.056	0.084	0.007	150.80
216	15.8	28.96	<11.52	4.88	4.57	<5.65	0.033	<10.54	0.05	0.081	0.007	155.46
217	17.0	<31.47	11.41	4.55	4.31	5.53	0.033	10.51	0.052	0.052	0.018	170.61
455 & 456	31.2	50.02	5.27	4.10	3.74	3.5	0.033	12.38	0.045	0.07	0.087	NA
467 & 468	44.1	64.06	14.26	7.28	5.49	54.3	0.053	13.53	0.078	155.34	0.361	172.91
471 & 472	50.1	<29.32	13.31	6.83	5.16	52.2	0.034	7.56	0.072	NA	0.113	127.24
475 & 476	59.1	77.08	13.16	6.73	4.70	53.2	0.018	14.59	0.076	143.33	0.111	93.70
479 & 480	73.1	48.17	12.05	5.35	3.26	51.1	0.012	12.26	0.058	122.65	0.121	57.03

7.0 Distribution

C. L. Bayer	730-2B, Rm. 2100
R. L. Brigmon	999-W, Rm. 323
B. T. Butcher	773-43A, Rm. 216
J. M. Clark	730-2B, Rm. 329
D. I. Kaplan	773-43A, Rm.215
A.K. Knox	773-42A, Rm. 231
P. C. McKinsey	999-W, Rm. 312
M. A. Phifer	773-42A, Rm. 252
A. L. Pishko	735-11A, Rm. 133
K. P. Crapse	773-43A, Rm. 212
J. A. Ross	730-2B, Rm. 3139
S. M. Serkiz	773A, Rm. B-121
R. P. Socha	730-2B, Rm. 3148
W. E. Stevens	773A, Rm. A-261
G. R. Wein	730-2B, Rm. 2064
STI, 4 copies	703-43A
WPT File	773-43A